Dynamics of DNA: B_I and B_{II} Phosphate Backbone Transitions

Michael Trieb, Christine Rauch, Bernd Wellenzohn, Fajar Wibowo, Thomas Loerting, and Klaus R. Liedl*

Institute of General, Inorganic and Theoretical Chemistry, University of Innsbruck, Innrain 52a, A-6020 Innsbruck, Austria

Received: October 11, 2003; In Final Form: December 10, 2003

In the present study, we try to determine if the dynamics of the B-DNA backbone phosphates (and especially their interconversions between their two distinct conformations B_I and B_{II}) are fast enough to be sufficiently sampled in the course of molecular dynamics simulations in the nanosecond time range. For this purpose, we performed twelve 10-ns simulations of the Drew−Dickerson dodecamer d(CGCGAATTCGCG)$_2$ to investigate the dynamics of B_I/B_{II} interconversion. We forced the DNA backbone angles ϵ and ζ with restraints to values that are characteristic for B_I and B_{II}, resulting in DNA double helices with all phosphates in the B_I or B_{II} substate. These restraints were removed after 10 ns, and unrestrained simulations at temperatures of 250, 275, 287.5, 300, and 325 K were performed for another 10 ns, which allowed us to analyze the dynamics of relaxation in detail. These simulations were compared to simulations of the undisturbed dodecamer at 250 and 300 K, as a reference for the equilibrated state. We found that the relaxation from the B_{II} state is considerably fast, with high rate constants, and is dependent on temperature. From this temperature dependence of the rate constants, we calculated the activation energy necessary for the B_{II} to B_I transition to be 2.5 kcal/mol. Half-life times of the B_{II} state derived from the relaxation process are in the range of 110−370 ps, which indicates that a simulation time of 10 ns is sufficiently long to investigate conformational transitions of the DNA backbone. The structures of the all-B_I DNA are more similar to structures found for the Drew−Dickerson dodecamer by X-ray crystallography than the all-B_{II} DNA. This fact is not astonishing, because the B_I conformation has been observed to be privileged. Nevertheless, both structures are quite different from canonical A- or B-DNA. That observation is revealing, because we expected the all-B_{II} DNA to be the transition state to canonical A-DNA or at least structurally very similar. Furthermore, we find that the relaxation of our rather-distorted starting structures is fast and, despite the large difference at the beginning, leads to a similar equilibrium, which, again, is similar to the undisturbed simulation.

1. Introduction

Understanding the mechanisms about how proteins or ligands interact with DNA are of major interest and importance. Besides interactions with the base edges in the minor and major groove of the DNA, contacts to the highly charged phosphates have been proven to be important for establishing close contacts and enabling sequence specificity.[1−7] Hence, the kinetics and thermodynamics of the DNA backbone are of major interest, especially because of the anionic nature of the backbone being one of the most important features. Here, we present a series of molecular dynamics (MD) simulations whose purpose is to elucidate dynamical interconversions between the two substates of phosphate groups in the DNA backbone. The two substates, called B_I and B_{II}, are defined by different conformations of the sugar phosphate backbone.[8] The changes are characterized by the angles ϵ and ζ of the DNA backbone or by the angle difference ($\epsilon - \zeta$). The change of the dihedral angle ϵ(C4′−C3′−O3′−P) is coupled to the dihedral angle ζ(C3′−O3′−P−O5′). In the more common B_I state, the corresponding ϵ and ζ angles are 120°−210° (trans) and 235°−295° (gauche), respectively. For B_{II}, ϵ = 210°−300° (gauche), and ζ = 150°−210° (trans). The angle difference ($\epsilon - \zeta$) is close to −90° for B_I and +90° for B_{II} phosphates.[2,7,9−19] With this study, we not only want to prove that the dynamics of the DNA backbone are fast and in the time scale of current MD simulations, but also that the overall distortions of the DNA structure that we introduced, corresponding to different starting structures for our MD simulation, are easily overcome during the course of the simulations and lead to trajectories that closely resemble canonical B-DNA. Hence, we are able to accurately investigate the interconversion of the phosphate substates that are important for interaction and recognition processes. For that purpose, we chose the Drew−Dickerson dodecamer d(CGCGAATTCGCG)$_2$, as it has been under extensive study because of its biological relevance both structurally and theoretically.[20−23] This dodecamer contains the recognition site of the EcoRI restriction enzyme and serves as a well-studied reference system. To the best of our knowledge, until now, no similar studies have been performed in which the DNA backbone was forced, by applying restraints, into a conformation where all phosphates in the phosphodiester backbone are in the B_{II} or B_I conformation. Although there is a wealth of studies that have investigated the DNA backbone, the question of interconversion times of the two B-DNA phosphate conformations, so far, have only been treated for single steps.[24−35] In the present study, we are looking at the interconversion from one state to the other, starting from a restrained system. For that purpose, we performed several 10-ns MD simulations of the EcoRI DNA dodecamer d(CGCGAATTCGCG)$_2$, with all phosphates forced into the B_I or B_{II}

* Author to whom correspondence should be addressed. E-mail: Klaus.Liedl@uibk.ac.at.

10.1021/jp037079p CCC: $27.50
Published on Web 01/22/2004

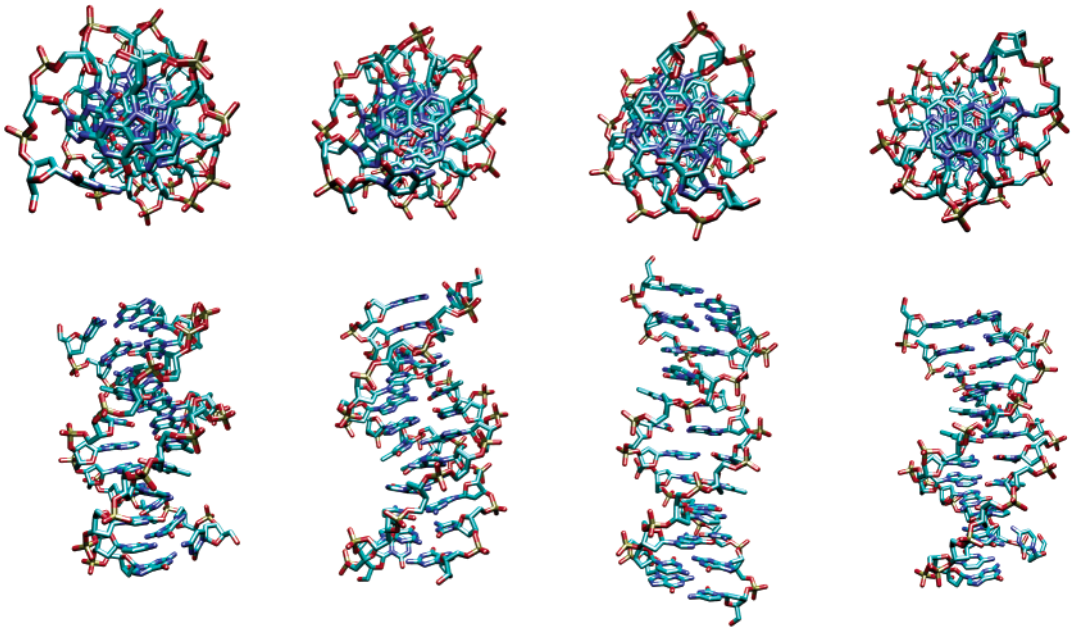

Figure 1. Averaged structures of the simulation results at 300 K. From left to right: B_I, restrained; B_I, relaxed, B_{II}, restrained; and B_{II}, relaxed. Top views are looking down the axis of the helix, and the bottom views are looking into the minor groove.

state by restraints. These restraints were acting onto the ϵ and ζ angles of the DNA backbone. After 10 ns, these restraints were removed and another 10 ns of unrestrained simulations were performed. This procedure was performed to investigate the relaxation times necessary to attain an equilibrium state of the backbone again. The structural convergence from the distorted starting points to structures that closely resemble canonical B-DNA was also attained very quickly. To obtain thermodynamic information, we performed the same relaxation calculations at five different temperatures. With our simulations, we are able to confirm MD simulations that had been performed previously[36] and gain a wealth of further insights into the dynamics of the DNA backbone. The present results stand in good agreement with results of MD simulations performed by our group on the influence of methylcytosine on the free energy of the B_I/B_{II} interconversion.[37]

2. Methods

The simulation of various sequences and lengths of DNA in an explicit solvent has been proven to be a valuable tool for a deeper understanding of the structural and dynamical properties of DNA in solution and its behavior in DNA−ligand or DNA−protein complexes. One major advantage of MD simulations is the possibility to study dynamical effects in the nanosecond time range, which is not accessible by other experimental methods. Therefore, gaining complementary information to experimental results is a major goal. All simulations were performed using the AMBER6 package.[38] Standard state-of-the-art simulation protocols were adapted for our needs.[16,17,39−41] The inclusion of the electrostatic long-range interactions via the particle mesh Ewald method[42,43] allows the accurate calculation of highly charged molecules such as DNA. Following these simulation protocols, it is possible to calculate stable trajectories in the nanosecond time range. The DNA structure of the Drew−Dickerson dodecamer has been thoroughly investigated by means of X-ray crystal structure, NMR, and MD simulations. We constructed a canonical B-DNA[44] with the sequence $d(CGCGAATTCGCG)_2$, using the program NUKIT. This structure was used as a reference and as the starting structure for our simulations. Each strand of the DNA has 11 PO_4^- anions. To achieve electroneutrality, 22 Na^+ ions were placed around the DNA. These ions were positioned using the program Xleap that was included in the AMBER6 package. Long-range interactions are taken into consideration, via the so-called particle mesh Ewald method, with a convergence criterion of 0.00001. The temperature is regulated by bath coupling, using the Berendsen algorithm,[45] and kept at the corresponding temperatures. Generally, other parameters of the simulation are a time step of 2 fs, constraints of 0.00005 Å for the SHAKE procedure (regarding all bonds that involve H atoms and a 9 Å nonbonded cutoff). In regard to a force field, we used the all-atom force field of Cornell et al.[46] with the modifications of Cheatham et al.[47] Counterions and water molecules are calculated explicitly using a TIP3P Monte Carlo water box[48] that requires a 12 Å solvent shell in all directions. The minimization was performed with harmonic restraints on the DNA and counterion positions. These restraints were relaxed stepwise and, at the end, a 500-step minimization without restraints was performed. A similar procedure was applied for the equilibration. The system was heated from 50 K to 300 K in 10 ps under constant-pressure conditions and harmonic restraints. After this procedure, the system was switched to constant temperature and pressure. Subsequently, the restraints were once again relaxed and finally an unrestrained 5-ps equilibration was performed. From this point, the respective simulations were performed.

Following the aforementioned procedure, we performed a simulation of the Drew−Dickerson dodecamer at 300 K for 20 ns (Figure 1). After 4.9 ns of this simulation, we took the resulting structure and applied restraints to force the phosphates into the B_I or B_{II} state. The restraints applied for the B_{II} simulation are defined by a lower bound of 215°, an upper bound of 295°, and force constants of 20 kcal/(mol rad^2) for the ϵ angles. For the dihedral angle ζ, a lower bound of 155° and an upper bound of 205°, with the same force constant as that previously mentioned, are used. The restraints were maintained for 10 ns of the simulation. Following this period, the restraints were removed and the simulation continued for another 10 ns, which shows the relaxation process of the backbone phosphates. During this time, the temperature was constantly maintained at 300 K.

From the aforementioned B_{II} restrained simulation at 300 K, we took the resulting structure after 10 ns, switched the temperature to 250, 275, 287.5, or 325 K, and maintained the new temperature and restraints on the system for another 200 ps. The restraints then were removed again and the relaxation process was observed for another 10 ns.

The simulations where all the phosphates were restrained into the B_I conformation were performed in a similar manner. For the B_I state, a lower bound of 125° and an upper bound of 205° was determined for the ϵ angle, and for the ζ dihedral angle, a lower bound of 240° and an upper bound of 290° is observed. Again, a force constant of 20 kcal/(mol rad^2) was used. The relaxation from the restrained states was observed at 250, 300, and 325 K, again for 10 ns. An additional reference simulation of the Drew−Dickerson dodecamer without any restraints, besides the simulation at 300 K, was also performed at 250 K for 10 ns. In total, more than 130 ns of simulation time contribute to our results.

Our major interest and purpose was to calculate the half-life of the two different B-DNA phosphodiester conformations. For that purpose, we used the change of the absolute number of B_{II} states as an indicator. The dodecamer has 22 phosphates and, thus, during application of restraints, a maximum number of 22 B_{II} conformations This maximum is not constantly reached during the restrained simulations, because the force constant was maintained at a reasonable value of 20 kcal/(mol rad^2) to prevent any artifacts and to leave a residual flexibility to the backbone. Therefore, the relaxation times were calculated by fitting an exponential function using the decrease gained from the simulations after removal of the restraints (see eq 1).

$$y = A_0 - \exp\left(-\frac{x}{k}\right) \tag{1}$$

A_0 is the only boundary parameter used for this fitting procedure; it indicates the maximal possible number of phosphates to be in the B_{II} state as an average over the restrained simulation time. Resulting from that fit (see Figure 1), we get the rate constants k of the relaxation process and, hence, the half-life times $\tau_{1/2}$ using eq 2.

$$\tau_{1/2} = \frac{\ln 2}{k} \tag{2}$$

That fitting of an exponential function was performed for all temperatures, and the resulting different temperature-dependent rate constants, where used for an Arrhenius plot of ln k versus $1/T$ (see Figure 8 later in this work). In eq 3, the relationship of the rate constant with the activation energy allows the activation energy to be calculated from the slope of the Arrhenius plot.[49]

$$k = A \exp\left(-\frac{E_a}{RT}\right) \tag{3}$$

Analysis tools for the resulting trajectories were carnal and ptraj, which are implemented in AMBER6.[38] Other tools that were used included RASMOL,[50] Molecular Dynamics Toolchest,[51] and VMD.[52]

3. Results

We are able to elucidate the thermodynamic and kinetic behavior of the DNA backbone through our investigations. We claim to have found relaxation and interconversion times on a remarkably short time scale (of just some hundreds of picoseconds), allowing sampling within simulation times of nanoseconds and also showing a high reproducibility. The thermodynamic results derived from our kinetic data let us conclude that the barrier of interconversion from the B_I conformation to the B_{II} conformation (2.5 kcal/mol) is small enough to be overcome, under normal conditions.

One major concern in our simulations is the question of if and when we can be certain that the obtained trajectories are in equilibrium, especially when we start from conformations that show reasonable distortions.[17,53,54] There are different indicators, not only for the stability of MD simulations but also for the similarity of two or more trajectories. Major indicators that we used for this purpose are the constancy of total energy and the root-mean-square deviation (RMSD) values calculated with respect to the starting or reference structures. Other important features that we examined included equilibrium values of groove width, hydration of the phosphates, occupation probability during the simulation of the B_{II} state for each phosphate and the different DNA interbase-pair and intrabase-pair parameters calculated with the program Dials and Windows. For more clarity, we want to split our results in three sections. First of all, we want to prove that we attained the corresponding equilibria during our simulations. The next point is the investigation of structural aspects of the distorted structures, in comparison to those of canonical A- and B-DNA, as well as the temporal change of DNA parameters during the relaxation process. Lastly, the major focus will lie on the kinetic and thermodynamic results that we can derive from our simulations.

3.1. Stability and Convergence of the Trajectories. One evidence for stable MD simulations is certainly the observation of changes in the total energy of the system. We observe that the total energy changes very quickly when the temperature is changed (within tens of picoseconds) and shows only slight changes when turning the restraints on or off (results not shown). Furthermore, no drift in energy is visible. The same is true for the temperature of the system. We find that the changes in temperature only need duration times on the order of picoseconds and switching from the restrained state to the unrestrained state does not show any effect. We find that, because of the high flexibility of DNA in solution, highly distorted structures such as an all-B_{II} conformation is still reasonable, although not naturally occurring. Examination of the RMSD changes during the course of the simulation time, except during changes in temperature or restraints, reveals no drift and just typical fluctuations around an averaged structure. To get an impression of the structural differences between the standard canonical A-DNA and B-DNA (Figure 2) and our distorted and relaxed structures, we were looking at the RMSD values. For that purpose, we calculated the averaged pdb structures from our trajectories using ptraj. Because these resulting structures show unrealistic bonding distances and angles, a minimization that leads to a difference in the normal gradient of energy of 1 kcal/(mol Å) prior to analyzes was performed. This averaging was performed for the entire trajectories with coordinate frames at every picosecond. The resulting structures can be seen in Figure 1. We calculated the RMSD values between all possible combinations of averaged structures with the program suppose that is included in the Nucleic Acid Builder (NAB).[55] The results are shown in Table 1.

We find that the averaged structures after relaxation, regardless of whether we start from an all-B_I or an all-B_{II} starting structure, are very similar to the undisturbed simulation results at 300 K. That is, the RMSD values are in the range of 0.9−1.7 Å. The B_{II} restrained states show a RMSD value of 3.5−4.1 Å, compared to the undisturbed simulation at 300 K, whereas

TABLE 1: Root-Mean-Square Deviation (RMSD) Values (in Ångstroms) Calculated with the Program Suppose[a]

RMSD[b]	(1)	(2)	(3)	(4)	(5)	(6)	(7)	(8)	(9)	(10)	(11)	(12)	(13)	(14)	(15)	(16)	(17)
(1) B_{II}rel 250 K																	
(2) B_{II}rel 275 K	0.9																
(3) B_{II}rel 287.5 K	0.8	1.1															
(4) B_{II}rel 300 K	1.1	1.2	1.1														
(5) B_{II}rel 325 K	1.7	1.8	1.6	1.7													
(6) B_{II}restr 250 K	3.2	3.3	3.5	3.7	3.9												
(7) B_{II}restr 275 K	3.6	3.7	3.9	4.1	4.2	0.7											
(8) B_{II}restr 287.5 K	3.1	3.3	3.3	3.6	3.7	0.8	1.0										
(9) B_{II}restr 300 K	2.9	3.1	3.2	3.4	3.5	0.9	1.3	0.9									
(10) B_{II}restr 325 K	3.2	3.4	3.5	3.7	3.8	0.9	1.1	1.0	0.9								
(11) $B_I$rel 250 K	1.7	1.8	1.6	1.7	2.1	3.2	3.6	3.1	2.8	3.1							
(12) $B_I$rel 300 K	2.0	1.6	2.0	2.2	2.5	3.9	4.2	3.9	3.7	4.0	2.9						
(13) $B_I$restr 250 K	2.1	2.2	2.0	2.0	2.7	3.8	4.2	3.6	3.4	3.7	1.3	3.3					
(14) $B_I$restr 300 K	2.3	2.1	2.2	2.1	2.7	4.7	5.0	4.7	4.6	4.8	3.3	1.9	3.5				
(15) A-DNA	5.5	5.4	5.2	5.0	5.4	8.0	8.4	7.9	7.7	8.0	5.8	5.4	5.6	4.5			
(16) B-DNA	1.8	1.9	2.0	2.2	2.6	2.4	2.8	2.3	2.1	2.4	1.5	2.9	1.8	3.5	6.3		
(17) unrestr 250 K[c]	1.3	1.4	1.1	1.3	1.9	4.0	4.3	3.9	3.7	4.0	2.3	2.1	2.4	1.7	4.8	2.5	
(18) unrestr 300 K[c]	1.2	0.9	1.2	1.2	1.7	3.7	4.1	3.7	3.5	3.8	2.2	1.4	2.5	1.7	5.0	2.4	1.3

[a] Shown is the lower part of a matrix of all pairwise RMSD values with the sequence of the first column being the same as in the first row, indicated by the numbers 1 to 18. [b] "Rel" denotes the relaxation and "restr" denotes the restrained simulations. [c] The data for "unrestr 250" and "unrestr 300 K" are those of the reference simulations without applying restraints at any time.

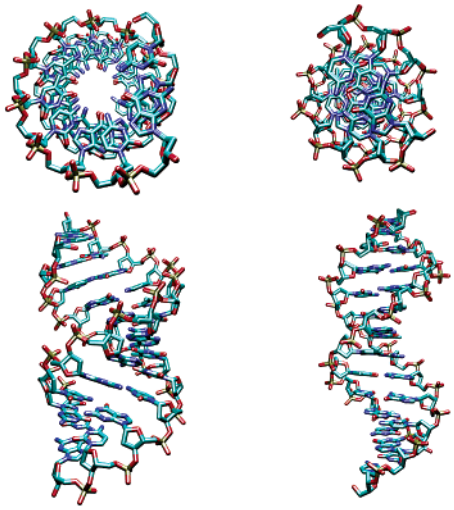

Figure 2. Comparison of the canonical A-DNA (left) and B-DNA (right) structures of the Drew−Dickerson dodecamer.

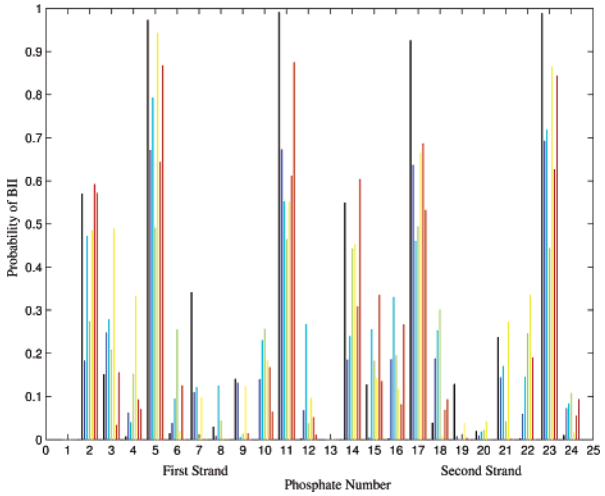

Figure 3. Probability of being in the B_{II} state, plotted per phosphate. From left to right: 250 K, 275 K, 287.5 K, 300 K, 325 K, and undisturbed simulation at 250 and 300 K. Phosphates P2−P12 are on the first strand of the DNA and phosphates P14−P24 are on the second strand. The similarity in the distribution of probability can be observed, as well as the symmetry of the two strands.

the B_I restrained states exhibit a somewhat lower RMSD value (1.7−2.5 Å), which can be explained by the fact that the major portion of the phosphates in the undisturbed simulation are already in the B_I state. Interestingly, when comparing the simulations of the Drew−Dickerson dodecamer at temperatures of 250 and 300 K with the relaxed structures at the different temperatures, a smaller difference in the RMSD values is observed, relative to that of the canonical B-DNA. We can definitely say that the B_{II} restrained states are rather far away from canonical A-DNA (RMSD = 7.7−8.4 Å) but, when relaxed, attain values that are comparable to the undisturbed simulations. Another proof for the convergence of the trajectories independent from starting structure to a similar structure can also be derived from the distinct distribution between the B_I conformation and the B_{II} conformation. In earlier studies, it has been shown that, for certain base-pair steps, one of the conformations is preferred over the other. Thus, our idea was to compare the patterns from the different simulations with each other and see if they show the same result. In Figure 3, we plotted the probability of all phosphates for all temperatures in the B_{II} relaxation simulations, as well as the two undisturbed reference simulations at 250 and 300 K, to be in the B_{II} state. We see that the expected pattern is indeed followed in all the simulations. Hence, this observation is another hint for the convergence of our calculations. Another point is the symmetry of the two DNA strands reflected in the symmetry of the pattern. When calculating the correlation coefficient for the probability for one phosphate and its corresponding symmetric counterpart at the other strand of being in the B_{II} conformation, we get correlations of at least 0.63; however, for most of the simulations, a correlation of >0.9 is observed.

3.2. Structural Influence of the DNA Backbone Conformations. We find it difficult to describe the structures of DNA with all phosphates in the B_{II} state, because this is not a naturally occurring structure and shows a great amount of distortion. In Figure 1, the averaged structures are shown. The primary differences to canonical A- or B-DNA can be ascribed to twist, X-displacement, and tilt values. We used the Molecular Dynamics Toolchest package[51] to calculate the DNA parameters. Also, the groove width is different between the two conformations. We concentrated on the difference between the B_{II} restrained

TABLE 2: Different DNA Forms and Their Corresponding Parameters

DNA form	XDP	YDP	INC	TIP	SHF	SLD	RIS	TLT	ROL	TWS
A-DNA[a]	−5.43	0.00	19.12	0.00	0.00	0.00	2.56	−0.00	0.00	32.70
B-DNA[a]	−0.71	0.00	−5.93	0.00	0.00	0.00	3.38	0.00	−0.00	36.00
B_I restr 300 K	−1.44	0.02	0.65	−0.20	0.01	−0.17	3.34	−0.04	3.95	33.53
B_{II} restr 300 K	1.30	−0.01	−0.46	0.15	0.02	0.10	3.43	0.32	−2.39	36.97
B_{II} rel 300 K	−0.44	1.24	−4.50	−8.31	0.12	−0.07	3.44	−3.12	3.24	32.59
unrestr 300 K	−0.69	−0.08	−1.03	0.37	0.00	−0.18	3.36	0.47	2.29	33.26

[a] Values taken from Neidle;[60] the other values are calculated with the Dials and Windows program as averages over all base-pair steps, omitting the terminal bases for the simulations at 300 K ("restr", restrained;, "rel", relaxed; "unrestr", reference simulation without ever applying restraints).

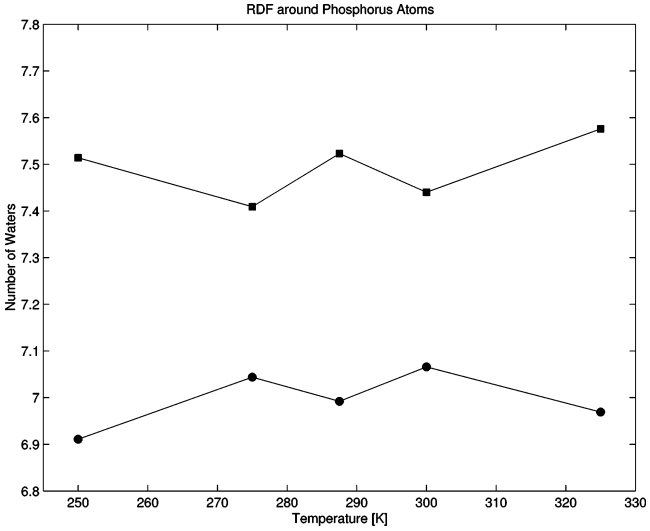

Figure 4. Differences in the number of water molecules in the first hydration shell around the P atoms in the backbone ((●) restrained values and (■) relaxed values).

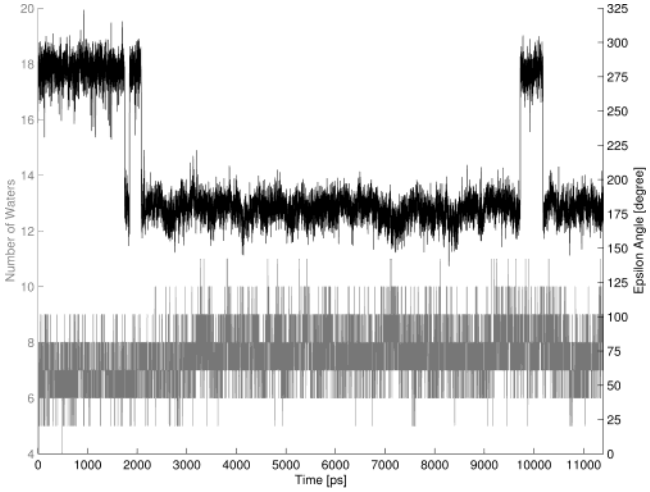

Figure 5. Simultaneous change of the dihedral angle ϵ at phosphate P3 and the hydration at a distance of 4.4 Å at 250 K. The number of water molecules is displayed on the left abscissa, and the backbone angle ϵ is shown on the right abscissa.

simulations at the different temperatures and the corresponding relaxed trajectories. In a previous study, the influence of the B_I/B_{II} transitions on changes in the hydration of B-DNA were investigated. We were also interested in the change of hydration during the course of relaxation. The phosphate backbone of the DNA is strongly hydrated; however, previous studies showed that these water molecules are kinetically labile.[32,56−59] Nevertheless, we were interested in changes in the number of water molecules around these phosphates. For that purpose, we calculated the radial distribution function of water around all P atoms of the backbone. We observed a dependence of the coordination number around the P atom from the substate. We also observed a minimum for the first hydration shell at 4.4 Å, with an average coordination number, over all temperatures, of 7.00 (standard deviation of 0.062) in the restrained state and 7.49 (standard deviation of 0.067) for the relaxed simulations (see Figure 4). The difference in hydration between the restrained simulations and the relaxed simulations around the phosphates shows an increase of hydration of 7.1%. To examine this fact more closely, we took the 250 K simulation and investigated the changes at selected phosphates. We observed that the change in the dihedral angle ϵ that brings the phosphate from a B_{II} state into a B_I conformation leads to an increase of water molecules around that position.[19,36] Exemplarily, the P3 phosphate is shown in Figure 5, where a change in ϵ from ∼280° to 180° is accompanied by an increase in the number of water molecules, from ∼6.9 to 7.7, in a distance of 4.4 Å. Transitions of the other phosphates show similar behavior. At temperatures of >250 K, the interconversion of the phosphate states is faster and, thus, the increase of hydration at specific sites and times is just observable as an increase in the average.

Interestingly, there are many DNA interbase-pair and intrabase-pair parameters that do not change when the restraints are applied (Table 2). All these values were calculated with Dials and Windows and averaged over all base-pair steps, leaving the terminal base pairs out, because these show end effects and a high flexibility, and, thus, would strongly influence the results. Some of the parameters are shown in Figure 6. For example, the rise changes only marginally, always remaining similar to that of canonical B-DNA, with a value of ∼3.4 Å. The same is true for the tilt and shift values. Major deviations are observed for roll, where, in the restrained state, it lies around −2.4°, whereas in the relaxed state, its value is 3.2°. Also, slide changes from 0.10 Å to −0.07 Å during relaxation. The most prominent differences are found with the twist and X-displacement parameters. The twist changes from ∼37.0° to 32.6° for the 300 K simulation. The X-displacement that is mainly responsible for the compacted structures in Figure 1 also is changing dramatically. For the B_{II} restrained simulations, we see that the base pairs are moved closer to the center of the helix axis, by ∼0.8 Å. This behavior can be clearly observed when one looks down the axis of the helix in Figure 1. In A-DNA, on the contrary, X-displacement is largely negative, pushing the base pairs away from the helical center and opening the view through the DNA (see Figure 2). Thus, we surmise that those parameters that do not change substantially when the restraints are applied are not (or not strongly) coupled to the DNA backbone.

3.3. Kinetic and Thermodynamic Results. For the calculation of our relaxation kinetics, we used the simple exponential function presented in eq 1. It is a relatively straightforward approach to evaluate this function with the only boundary parameter A_0, which represents the number of B_{II} states at the starting time (Figure 7). The rate constant (k) can be derived

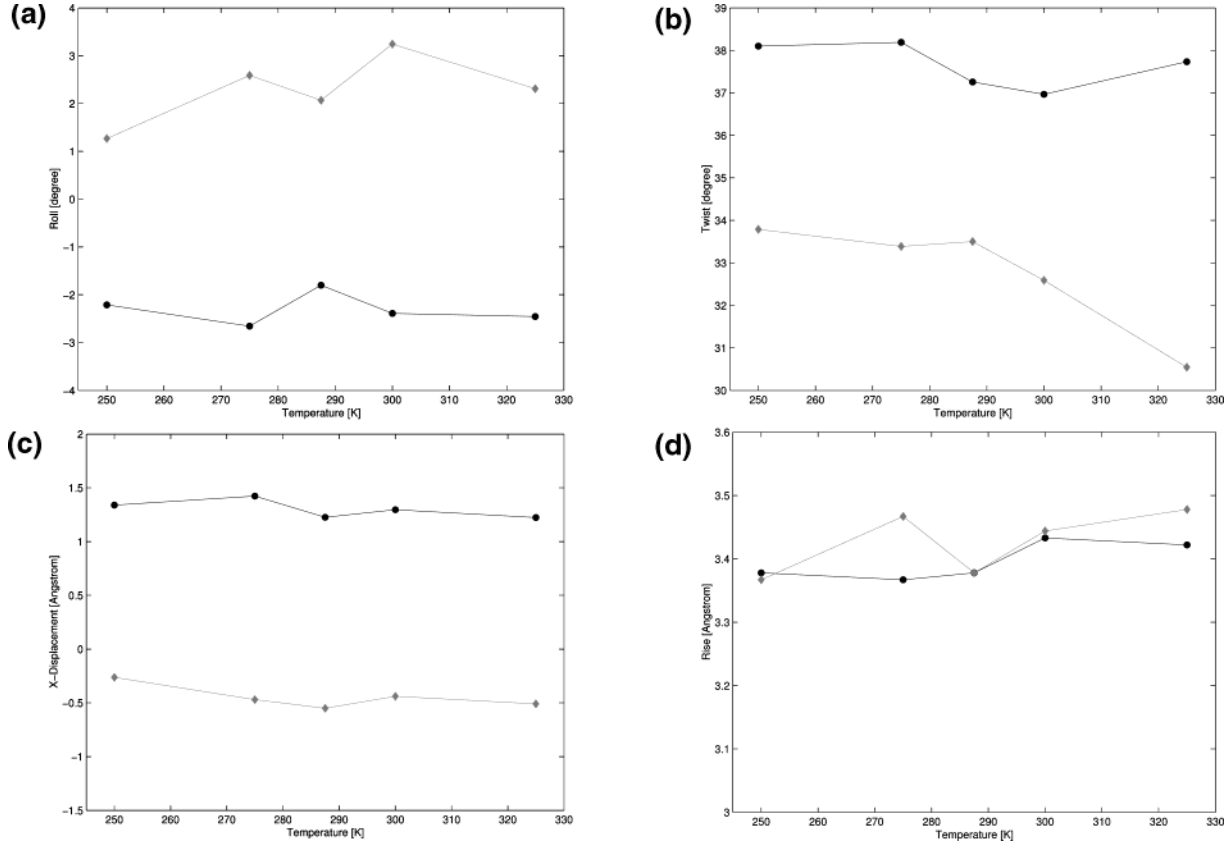

Figure 6. DNA parameters (a) roll, (b) twist, (c) X-displacement, and (d) rise. Values are plotted for all temperatures. Legend for each figure is as follows: (●) restrained values and (♦) relaxed values.

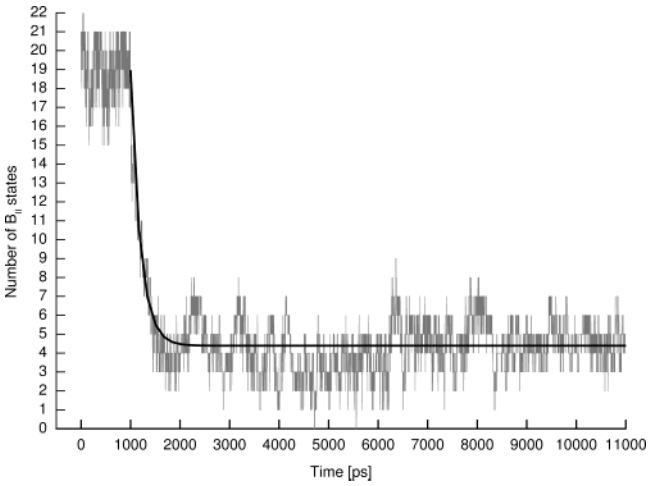

Figure 7. Exemplary display of the simulation of the B_{II} relaxed simulation at 300 K. The first nanosecond stems from the restrained simulation, whereas after that, the relaxation is observed for 10 ns. On the abscissa, the total number of B_{II} states is plotted. In addition, the exponential function used to calculate the rate constant in this case is shown as a black line (the first nanosecond was not used for the fitting process).

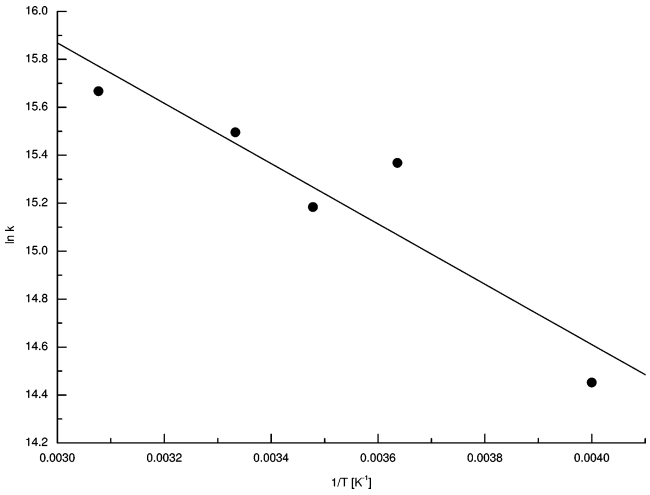

Figure 8. Arrhenius plot of ln k versus $1/T$ for all temperatures, which allows calculation of the activation energy.

TABLE 3: Resulting Rate Constants for the Different Temperatures and the Half-Life Times for the Relaxation Process

temperature, T (K)	rate constant, k (s^{-1})	half-life time, $\tau_{1/2}$ (ps)
250	1.89×10^6	367
275	4.72×10^6	147
287.5	3.93×10^6	177
300	5.37×10^6	129
325	6.37×10^6	109

directly from that plot, and we have observed k values ranging from 1.89×10^6 s^{-1} at 250 K to 6.37×10^6 s^{-1} at 325 K (Table 3). The rate constants are related to the half-life times ($\tau_{1/2}$) through eq 2. Thus, we find relaxation half-life times of $\tau_{1/2} =$ 109 ps at the highest temperature and $\tau_{1/2} = 367$ ps at the lowest temperature. This allows us to reach the following conclusion: this fast relaxation process is not only observable during the time course of our simulations in general, but also reaches equilibrium at temperatures usually chosen for MD within times that are 5−10 times greater than the half-life time (that is, 500−1500 ps).[61,62] Another important item of information that can be taken from our calculations is the activation energy for the B_{II}-to-B_I transition (Figure 8). According to eq 3 and the Arrhenius plot, we get an activation energy of 2.5 kcal/mol.

4. Summary and Conclusion

We have determined that the relaxation from the B_{II} state is considerably fast, with high rate constants, and is dependent on temperature. Furthermore, the activation energy necessary for this process is low enough to be easily overcome. Relaxations from the B_I state were not suitable for calculation of the half-life times, because this state is too similar to the undisturbed and preferred phosphate conformation. The structures of the all-B_I DNA seem to be more similar to those observed by X-ray crystallography than the all-B_{II} state. Nevertheless, both structures are quite different from canonical A- or B-DNA.

Acknowledgment. This work was supported by a grant from the Austrian Science Fund (Grant No. P16176-TPH), for which we are grateful. Special thanks goes to Drs. A. F. Voegele and M. J. Loferer for fruitful discussions.

References and Notes

(1) Tisne, C.; Delepierre, M.; Hartmann, B. *J. Mol. Biol.* **1999**, *293*, 139−150.
(2) Bertrand, H. O.; Ha-Duong, T.; Fermandjian, S.; Hartmann, B. *Nucleic Acids Res.* **1998**, *26*, 1261−1267.
(3) Wellenzohn, B.; Flader, W.; Winger, R. H.; Hallbrucker, A.; Mayer, E.; Liedl, K. R. *Biochemistry* **2002**, *41*, 4088−4095.
(4) Cramer, P.; Larson, C. L.; Verdine, G. L.; Müller, C. W. *EMBO J.* **1997**, *16* (23), 7078−7090.
(5) Wecker, K.; Bonnet, M. C.; Meurs, E. F.; Delepierre, M. *Nucleic Acids Res.* **2002**, *30* (20), 4452−4459.
(6) Wellenzohn, B.; Flader, W.; Winger, R. H.; Hallbrucker, A.; Mayer, E.; Liedl, K. R. *J. Am. Chem. Soc.* **2001**, *123*, 5044−5049.
(7) Rüdisser, S.; Hallbrucker, A.; Mayer, E. *J. Am. Chem. Soc.* **1997**, *119*, 12251−12256.
(8) Schneider, B.; Neidle, S.; Berman, H. M. *Biopolymers* **1997**, *42*, 113−124.
(9) Fratini, A. V.; Kopka, M. L.; Drew, H. R.; Dickerson, R. E. *J. Biol. Chem.* **1982**, *257*, 14686−14707.
(10) Gupta, G.; Bansal, M.; Sasiskharan, V. *Proc. Natl. Acad. Sci., U.S.A.* **1980**, *77*, 6486−6490.
(11) Privé, G. G.; Heinemann, U.; Chandrasegaran, S.; Kan, L.-S.; Kopka, M. L.; Dickerson, R. E. *Science* **1987**, *238*, 498−504.
(12) Cruse, W. B. T.; Salisbury, S. A.; Brown, T.; Cosstick, R.; Eckstein, F.; Kennard, O. *J. Mol. Biol.* **1986**, *192*, 891−905.
(13) Shindo, H.; Fujiwara, T.; Akutsu, H.; Masumoto, U.; Shimidzu, M. *J. Mol. Biol.* **1984**, *174*, 221−229.
(14) Sklenar, V.; Bax, A. *J. Am. Chem. Soc.* **1987**, *109*, 7525−7526.
(15) Gorenstein, D. G. *Chem. Rev.* **1994**, *94*, 1315−1338.
(16) Winger, R. H.; Liedl, K. R.; Rüdisser, S.; Pichler, A.; Hallbrucker, A.; Mayer, E. *J. Phys. Chem. B* **1998**, *102*, 8934−8940.
(17) Young, M. A.; Ravishanker, G.; Beveridge, D. L. *Biophys. J.* **1997**, *73*, 2313−2336.
(18) Cheatham, T. E.; Kollman, P. A. *J. Am. Chem. Soc.* **1997**, *119*, 4805−4825.
(19) Pichler, A.; Rüdisser, S.; Mitterböck, M.; Huber, C. G.; Winger, R. H.; Liedl, K. R.; Hallbrucker, A.; Mayer, E. *Biophys. J.* **1999**, *77*, 398−409.
(20) Dickerson, R. E.; Drew, H. R. *J. Mol. Biol.* **1981**, *149*, 761−786.
(21) Drew, H. R.; Dickerson, R. E. *J. Mol. Biol.* **1981**, *151*, 535−556.
(22) Wing, R.; Drew, H.; Takano, T.; Broka, C.; Tanaka, S.; Itakura, K.; Dickerson, R. E. *Nature* **1980**, *287*, 755−758.
(23) Drew, H. R.; Wing, R. M.; Takanao, T.; Broka, C.; Tanaka, S.; Itakura, K.; Dickerson, R. E. *Proc. Natl. Acad. Sci., U.S.A.* **1981**, *78*, 2179−2183.
(24) Berman, H. M. *Biopolymers* **1997**, *44*, 23−44.
(25) Calladine, C. R.; Drew, H. R. *Understanding DNA*; Academic Press: San Diego, CA, 1997.
(26) Foloppe, N.; MacKerell, A. D. *J. Phys. Chem. B* **1999**, *103*, 10955−10964.
(27) Hamelberg, D.; Williams, L. D.; Wilson, W. D. *Nucleic Acids Res.* **2002**, *30* (16), 3615−3623.
(28) Hogan, M. E.; Jardetzky, O. *Proc. Natl. Acad. Sci., U.S.A.* **1979**, *76*, 6341−6345.
(29) Packer, M.; Hunter, C. *J. Mol. Biol.* **1998**, *280*, 407−420.
(30) Schuerman, G. S.; Van Meervelt, L. *J. Am. Chem. Soc.* **2000**, 232−240.
(31) Wellenzohn, B.; Flader, W.; Winger, R. H.; Hallbrucker, A.; Mayer, E.; Liedl, K. R. *Nucleic Acids Res.* **2001**, *29* (24), 5036−5043.
(32) Feig, M.; Pettitt, B. M. *J. Mol. Biol.* **1999**, *286*, 1075−1095.
(33) McConnell, K. J.; Nirmala, R.; Young, M. A.; Ravishanker, G.; Beveridge, D. L. *J. Am. Chem. Soc.* **1994**, *116*, 4461−4462.
(34) van Dam, L.; Levitt, M. H. *J. Mol. Biol.* **2000**, *304*, 541−561.
(35) Hartmann, B.; Piazzola, D.; Lavery, R. *Nucleic Acids Res.* **1993**, *21*, 561−568.
(36) Flader, W.; Wellenzohn, B.; Winger, R. H.; Hallbrucker, A.; Mayer, E.; Liedl, K. R. *J. Phys. Chem. B* **2001**, *105*, 10379−10387.
(37) Rauch, C.; Trieb, M.; Wellenzohn, B.; Loferer, M.; Voegele, A.; Wibowo, F. R.; Liedl, K. R. *J. Am. Chem. Soc.* **2003**, *125*, 14990−14991.
(38) Case, D. A.; Pearlman, D. A.; Caldwell, J. W.; Cheatham, T., III; Ross, W. S.; Simmerling, C. L.; Darden, T. A.; Merz, K. M.; Stanton, R. V.; Cheng, A. L.; Vincent, J. J.; Crowley, M.; Tsui, V.; Radmer, R. J.; Duan, Y.; Pitera, J.; Massova, I.; Seibel, G. L.; Singh, U. C.; Weiner, P. K.; Kollman, P. A. *AMBER 6*. University of California, San Francisco, CA, 1999.
(39) Young, M. A.; Jayaram, B.; Beveridge, D. L. *J. Am. Chem. Soc.* **1997**, *119*, 59−69.
(40) de Souza, O. N.; Ornstein, R. L. *Biophys. J.* **1997**, *72*, 2395−2397.
(41) de Souza, O. N.; Ornstein, R. L. *J. Biomol. Struct. Dyn.* **1997**, *14*, 607−611.
(42) York, D. M.; Wlodawer, A.; Pedersen, L. G.; Darden, T. A. *Proc. Natl. Acad. Sci., U.S.A.* **1994**, *91*, 8715−8718.
(43) Cheatham, T. E.; Kollman, P. A. *J. Mol. Biol.* **1996**, *259*, 434−444.
(44) Arnott, S.; Campbell-Smith, P. J.; Chandrasekaran, R. *CRC Handbook of Biochemistry and Molecular Biology*. CRC Press: Boca Raton, FL, 1976.
(45) Berendsen, H. J. C.; Postma, J. P. M.; Van Gunsteren, W. F.; DiNola, A.; Haak, J. R. *J. Chem. Phys.* **1984**, *81*, 3684−3690.
(46) Cornell, W. D.; Cieplak, P.; Bayly, C. I.; Gould, I. R.; Merz, K. M.; Ferguson, D. M.; Spellmeyer, D. C.; Fox, T.; Caldwell, J. W.; Kollman, P. A. *J. Am. Chem. Soc.* **1995**, *117*, 5179−5197.
(47) Cheatham, T. E.; Cieplak, P.; Kollman, P. A. *J. Biomol. Struct. Dyn.* **1999**, *16*, 845−862.
(48) Jorgensen, W. L. *J. Am. Chem. Soc.* **1981**, *103*, 335−340.
(49) Fersht, A. *Structure and Mechanism in Protein Science: A Guide to Enzyme Catalysis and Protein Folding*. W. H. Freeman: New York, 1999.
(50) Sayle, R. *RasMol 2.6*; Glaxo Wellcome Medicines Research Centre: Hertfordshire, U.K., 1995.
(51) Ravishanker, G.; Swaminathan, S.; Beveridge, D.; Lavery, R.; Sklenar, H. J. *J. Biomol. Struct. Dyn.* **1989**, *6*, 669−699.
(52) Humphrey, W.; Dalke, A.; Schulten, K. *J. Mol. Graphics* **1996**, *14* (1), 33−38.
(53) Genest, D. *Biopolymers* **1996**, *38*, 389−399.
(54) Feig, M.; Pettitt, B. M. *Biophys. J.* **1998**, *75*, 134−149.
(55) Macke, T.; Case, D. A. *Molecular Modeling of Nucleic Acids: Modeling Unusual Nucleic Acid Structures*. American Chemical Society: Washington, DC, 1998.
(56) Falk, M.; Hartman, K.; Lord, R. *J. Am. Chem. Soc.* **1962**, *84*, 3843−3846.
(57) Denisov, V. P.; Carlstöm, G.; Venu, K.; Halle, B. *J. Mol. Biol.* **1997**, *268*, 118−136.
(58) Duan, Y.; Wilkosz, P.; Crowley, M.; Rosenberg, J. M. *J. Mol. Biol.* **1997**, *272*, 553−572.
(59) Schneider, B.; Patel, K.; Berman, H. M. *Biophys. J.* **1998**, *75*, 2422−2434.
(60) Neidle, S. *Oxford Handbook of Nucleic Acid Structure*. Oxford University Press: Oxford, U.K., 1999.
(61) Brauns, E. B.; Madaras, M. L.; Coleman, R. S.; Murphy, C. J.; Berg, M. A. *J. Am. Chem. Soc.* **1999**, *121*, 11644−11649.
(62) Brauns, E. B.; Madaras, M. L.; Coleman, R. S.; Murphy, C. J.; Berg, M. A. *Phys. Rev. Lett.* **2002**, *88* (15), 1581011−1581014.